

# Probability-Biased Attention over Directed Bipartite Graphs for Long-Tail ICD Coding

Tianlei Chen<sup>b</sup>, Yuxiao Chen<sup>b</sup>, Yang Li<sup>a,b</sup>, Feifei Wang<sup>a,b,\*</sup>

<sup>a</sup>*Center for Applied Statistics, Renmin University of China, Beijing, 100872, China*

<sup>b</sup>*School of Statistics, Renmin University of China, Beijing, 100872, China*

---

## Abstract

Automated International Classification of Diseases (ICD) coding aims to assign multiple disease codes to clinical documents, constituting a crucial multi-label text classification task in healthcare informatics. However, the task is challenging due to its large label space (10,000 to 20,000 codes) and long-tail distribution, where a few codes dominate while many rare codes lack sufficient training data. To address this, we propose a learning method that models fine-grained co-occurrence relationships among codes. Specifically, we construct a Directed Bipartite Graph Encoder with disjoint sets of common and rare code nodes. To facilitate a one-way information flow, edges are directed exclusively from common to rare codes. The nature of these connections is defined by a probability-based bias, which is derived from the conditional probability of a common code co-occurring given the presence of a rare code. This bias is then injected into the encoder's attention module, a process we term Co-occurrence Encoding. This structure empowers the graph encoder to enrich rare code representations by aggregating latent comorbidity information reflected in the statistical co-occurrence of their common counterparts. To ensure high-quality input to the graph, we utilize a large language model (LLM) to generate comprehensive descriptions for codes, enriching initial embeddings with clinical context and comorbidity information, serving as external knowledge for the statistical co-occurrence relationships in the code system. Experiments on three automated ICD coding

---

\*Corresponding author

*Email addresses:* [chentianlei@ruc.edu.cn](mailto:chentianlei@ruc.edu.cn) (Tianlei Chen),  
[cyx2023201820@ruc.edu.cn](mailto:cyx2023201820@ruc.edu.cn) (Yuxiao Chen), [yang.li@ruc.edu.cn](mailto:yang.li@ruc.edu.cn) (Yang Li),  
[feifei.wang@ruc.edu.cn](mailto:feifei.wang@ruc.edu.cn) (Feifei Wang)

benchmark datasets demonstrate that our method achieves state-of-the-art performance with particularly notable improvements in Macro-F1, which is the key metric for long-tail classification.

*Keywords:* ICD Coding, Multi-label Text Classification, Long-tail, Graph Transformer, Large Language Models

---

## 1. Introduction

The International Classification of Diseases (ICD<sup>1</sup>) is a healthcare classification system maintained by the World Health Organization (WHO) that provides a unique code for each diagnose or procedure. Although widely adopted, the manual process of assigning ICD codes to clinical text is time-consuming, error-prone, and expensive. Automated ICD coding is typically framed as a multi-label text classification task [1], but it presents a significant challenge: a small subset of codes, such as those for chronic conditions like diabetes, dominates the frequency distribution. Meanwhile, the majority of codes, often corresponding to rare diseases or nuanced complications, appear infrequently, creating a long-tail distribution. In the MIMIC-IV-ICD-10 dataset, for example, over 70% of its 26,096 distinct codes occur fewer than 10 times [2]. This severe data imbalance hinders the ability of data-driven classification models to learn meaningful semantic representations for these rare codes.

A primary strategy for automated ICD coding is leveraging co-occurrence relationship (see Figure 1) to capture complicated correlations among codes. Cao et al. [3], Luo et al. [4], and Wang et al. [5] model these correlations via graph networks, motivated by comorbidity as the clinical foundation underlying statistical co-occurrence [6]. However, these methods critically oversimplify co-occurrence relationships into binary connections, ignoring fine-grained statistical information, such as conditional probabilities that refine the correlation between rare and common codes, limiting representation enhancement especially for data-scarce rare codes.

Another line of research focuses on exploring external knowledge to enrich code semantics. Representative approaches like MSMN [7], KEPT [8] and MSAM [9] expand code representations by aligning code names with synonyms from medical ontologies (e.g., UMLS, Wikidata). While this leverages

---

<sup>1</sup><https://www.who.int/standards/classifications/classification-of-diseases>

Clinical Document	ICD Codes with Names
<p> <b>First Name</b>3 (LF) 2751 </p> <p> <b>Date of Birth:</b> 2118-6-9 </p> <p> <b>Sex:</b> F..... </p> <p> <b>Social History:</b> Drinks 2 pints per day, most recent drink on Sunday per the pt..... </p> <p> <b>Brief Hospital Course:</b> In the MICU, Lactate, AG acidosis trended down ..... Patient was extubated on hospital day 2 and transferred to the floor, where her ammonia and valproic acid levels continued to decline..... </p> <p> ..... </p>	<p> <b>270.6:</b> Urea cycle disorder </p> <p> <b>276.2:</b> Acidosis </p> <p> <b>96.04:</b> Intratracheal intubations </p> <p> ..... </p>

Figure 1: An example of a clinical document assigned the co-occurring codes “Urea cycle disorder”, “Acidosis”, and others. “Acidosis” is often triggered by “Urea cycle disorder”, as toxic ammonia buildup disrupts cellular metabolism.

lexical variations, a critical limitation persists: synonym expansions frequently exhibit semantic homogeneity with the original code names. To illustrate, the synonyms “disorder of urea cycle metabolism, unspecified” and “disorder of the urea cycle metabolism, nos” both belong to ICD code 270.6, which has the name “urea cycle disorder”. Consequently, such methods are only marginally effective at injecting meaningful knowledge to enhance code representations, leaving significant room for improvements in classification performance.

Additionally, some studies have designed complex multi-stage frameworks. To manage the vast label space of the ICD code system, methods such as GPsoap [10] and TwoStage [11], typically involve a pipeline of discrete steps like retrieving and re-ranking candidate codes. Notably, these frameworks can be combined with other high-performing end-to-end models to achieve better performance.

In this work, we propose a learning method that utilizes fine-grained co-occurrence relationships to enhance rare code representations. Specifically, we construct a Directed Bipartite Graph Encoder with two disjoint node sets: common codes and rare codes. The edges between them are directed exclusively from common to rare codes, with nature identified by conditional probability—the likelihood of a common code occurring given the presence of a specific rare code. We discretize the continuous probability values into bins, which then index a learnable bias in an attention module, a process we term “Co-occurrence Encoding”. This graph encoder enhances the representation learning of rare codes by enabling them to aggregate latent comorbidity

information from their co-occurring common counterparts. To create high-quality input to the graph, we leverage a specialized LLM prompt to generate comprehensive ICD code descriptions. This approach moves beyond the simple synonyms used in prior work by incorporating detailed clinical contexts and valuable comorbidity information, underpinning the statistical co-occurrence analysis with external knowledge. After encoding code representations, we employ a multi-label attention to get final prediction for each document. We call our model **ProBias**<sup>2</sup> (derived from the core component “**Probability-based Bias**” in our proposed Directed Bipartite Graph Encoder). Experiments show that these measures enable our approach to achieve state-of-the-art (SOTA) performance across three benchmark datasets, particularly on metrics sensitive to long-tail distributions.

Our work makes three key contributions:

- First, to the best of our knowledge, this is the first study to enhance rare code representations by directed leveraging information from their co-occurring common counterparts.
- Second, we introduce a novel Directed Bipartite Graph Encoder that integrates a tailored attention mechanism with a probability-based bias. This structure effectively models and utilizes statistical co-occurrence relationship to facilitate information flow from common to rare codes, effectively addressing the long-tail challenge.
- Third, we strategically employ a Large Language Model (LLM) to generate comprehensive descriptions for ICD codes, including clinical context and comorbidity information, effectively augmenting the initial code embeddings with domain-specific knowledge before they are processed by our graph encoder.

The remainder of this paper is organized as follows: Section 2 reviews related work, Section 3 details our methodology, Section 4 presents experiments, and Section 5 concludes with limitations and future directions.

---

<sup>2</sup>The code for our ProBias model is publicly available at <https://github.com/ChTian1EI/ProBias-for-ICD-Coding>.

## 2. Related work

### 2.1. Co-occurrence Relationships Extraction

Many existing works utilize co-occurrence among codes to extract their correlations. HyperCore [3] was the first work to exploit code co-occurrence relationships for automatic ICD coding. It defines the co-occurrence using an adjacency matrix, where the edge weights are directly determined by the raw co-occurrence counts between codes, and this structural information is then encoded by a Graph Convolutional Network (GCN). Other approaches have built upon this concept with different strategies for modeling co-occurrence. For instance, Wang et al. [5] propose a method that binarizes co-occurrence relationships by representing the presence or absence of code pairs. These binarized features are then incorporated into a graph transformer model. In another direction, CoRelation [4] integrates the ICD code ontology with the co-occurrence graph to construct a simplified, contextualized graph for each note. To manage complexity, this graph’s nodes are reduced by only selecting the top-K codes with the highest initial prediction probabilities for one node set, while using coarse-grained major code categories for the other.

### 2.2. External Knowledge Exploration

To enhance the semantic representation of ICD codes, a primary strategy involves extending code names with information from external medical knowledge bases. One prominent approach is to extract synonyms. For instance, MSMN [7] aligns ICD codes with concepts in UMLS to gather synonyms and proposes a multi-synonym attention mechanism where each synonym acts as a separate query to extract relevant text snippets from the clinical note. Further extending this idea, MSAM [9] expands the knowledge sources to include Wikidata and Wikipedia. Recognizing that synonym lists can be repetitive, it also employs a selection algorithm to choose a more representative subset of synonyms for each code. Other works integrate multiple types of knowledge simultaneously. For example, KEPT [8] integrates a pre-trained language model with three domain-specific knowledge sources: code hierarchy, synonyms, and abbreviations.

### 2.3. Graph Models Utilization

Graph models play a crucial role in automatic ICD coding. For instance, Graph Convolutional Networks (GCNs) [12] have been adopted by ZAGCNN [13], MSATT-KG [14], and HyperCore [3]. More recently, Transformer-based

graph models have gained increasing attention. For example, CoRelation [4] employs a graph Transformer [15] to model the interactions between codes on its constructed simplified graph. Similarly, Wang et al. [5] leverage Graphormer [16] to extract the co-occurrence relationships simply based on the connectivity between any two codes.

A key innovation of the Transformer-based graph model Graphormer [16] is how it injects structural information into the attention module. Its "Spatial Encoding" component adds a learnable bias to the attention score between any two nodes. This bias is specifically indexed by the shortest path distance (SPD) between the nodes, allowing the model to incorporate graph topology directly into its calculations. Our work adapts this core principle for the specific challenges of ICD coding.

### 3. Method

For automated ICD coding, existing methods commonly treat it as a multi-label text classification problem. Given a clinical document (e.g., discharge summary)  $X = \{x_i : i \in \{1, 2, \dots, T\}\}$ , where  $T$  represents the potentially thousands of tokens that compose  $X$ . Each document  $X$  is associated with a ground-truth label set  $L = \{l_i : i \in \{1, 2, \dots, M\}\}$ , where  $M$  indicating the number of labels. The objective of automated ICD coding is to predict the label set  $L$  for document  $X$ . Note that, each ICD code represents either a diagnose or a procedure, serving as the task’s label, and typically comes with an original name.

In this section, we introduce the technical details of the proposed method. The pipeline is illustrated in Figure 2.

#### 3.1. Documents Encoding

To start with, we choose GatorTron [17] as the foundational Language Model (LM) for clinical documents encoding. GatorTron is an encoder model pre-trained on medical corpora, which is publicly available in the NVIDIA NGC<sup>3</sup> Catalog and also through the HuggingFace<sup>4</sup> library.

As noted in [18], Chunk encoding effectively mitigates the challenges language models encounter when processing lengthy inputs. Given the substantial length of clinical documents, we adopted the approach in [9], partitioning each

---

<sup>3</sup><https://catalog.ngc.nvidia.com/>

<sup>4</sup><https://huggingface.co/UFNLP/gatortron-base>

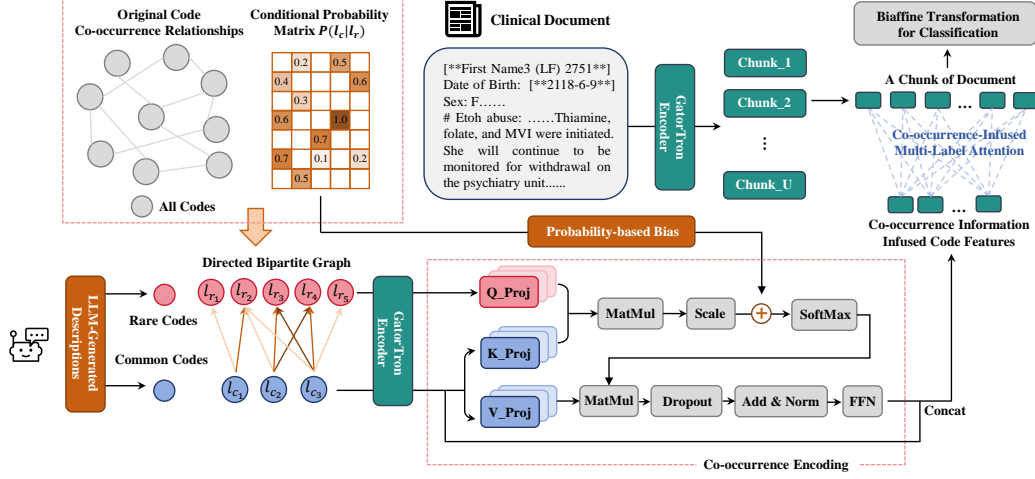


Figure 2: The pipeline of our proposed model, ProBias. The process begins with generating comprehensive code descriptions via a Large Language Model (LLM). Next, a Directed Bipartite Graph is constructed based on the Original Code Co-occurrence Relationships and Conditional Probability Matrix, in which arrows of different colors denote different probabilities. The information flow within this graph is governed by our Co-occurrence Encoding, which injects a learnable bias derived from the Conditional Probability Matrix into the attention scores. The final classification is then performed using a Co-occurrence-Infused Multi-Label Attention mechanism.

document into  $U$  overlapped chunks and processing each chunk independently using GatorTron. This approach circumvents the token limit of the standard Transformer encoder, enabling effective analysis of lengthy clinical documents. Specifically, for a document  $X = \{X_1, X_2, \dots, X_U\}$  that has been divided into chunks, where each chunk  $X_u = \{w_1^u, w_2^u, \dots, w_T^u\}$ ,  $U$  has a fixed length of  $T = 512$  tokens. we employ the GatorTron model to derive its representation:

$$H^u = \text{GatorTron}(X_u) \in \mathbb{R}^{T \times d} \quad (1)$$

Here,  $d$  represents the dimension of the hidden layer.

### 3.2. Initial Code Embeddings

To generate the code descriptions, we employ GPT-4o, a brilliant large language model from OpenAI. Its advanced capabilities in semantic understanding, instruction-following, and its extensive knowledge base are crucial for our task, which requires generating highly structured and medically accurate descriptions. To ensure consistency and reproducibility in the output,

we set the temperature parameter to a low value (0.2). The model is guided by a structured prompt template designed to produce a comprehensive description for each ICD code, covering clinical contexts, procedural methods, and comorbidity information (see Figure 3 for prompt details and Figure 4 for an example of description).

```

"""
You are a clinical terminologist with expertise in ICD-10 coding.
When provided with ICD-10 code titles, generate for EACH code:
1. Comprehensive description covering:
  - Code definition and clinical context
  - Primary indications/pathologies
  - Procedural methods (if applicable)
2. Comorbidity information including:
  - Top 1-3 complications and underlying causes
  - Pathophysiological mechanisms linking complications

STRICT OUTPUT FORMAT for EACH CODE:
[ICD-10 code title]: [The code title provided in the input]
[comprehensive description]: [A comprehensive paragraph covering the code's definition, clinical
context, primary indications/pathologies, and applicable procedural methods, written in a clinical
tone.];
[comorbidity information]: [A detailed paragraph describing the top 1-3 complications, underlying
causes, and the pathophysiological mechanisms linking them.];

=====

Input code titles:
{code_titles}
"""

```

Figure 3: A structured prompt template designed to produce a comprehensive description for each ICD code, covering clinical contexts, procedural methods, and comorbidity information.

The resulting descriptions are then encoded using the GatorTron model [17] to obtain the initial code embeddings:

$$V_i = \text{GatorTron}(d_i)[\text{CLS}] \quad (2)$$

Here,  $d_i$  denotes the description of the  $i$ -th code  $l_i$ , where  $i \in \{1, 2, \dots, N\}$  and  $N$  is the total number of codes. These initial code embeddings are then input into the Directed Bipartite Graph Encoder, serving as the basis for capturing fine-grained co-occurrence relationships. Notably, the GatorTron model for these code descriptions remains untrained to mitigate significant GPU memory usage, given the large number of codes.



<p><b>Code's Original Name</b></p> <p><b>270.6:</b> Urea cycle disorder</p>
<p><b>LLM generated description</b></p> <p>"<b>COMPREHENSIVE_DESC</b>": "Disorders of urea cycle metabolism are <b>genetic conditions</b> that result in the body's inability to effectively remove ammonia, a waste product of protein metabolism. This can lead to <b>hyperammonemia</b>, which is <b>toxic to the brain</b>. Clinical context includes conditions such as <b>ornithine transcarbamylase deficiency</b> and <b>citrullinemia</b>. Procedural methods for diagnosis include <b>genetic testing</b>, <b>plasma ammonia levels</b>, and <b>enzyme assays</b>. Primary indications/pathologies involve lethargy, vomiting, and neurological symptoms. Key risks/complications include <b>brain damage</b>, <b>coma</b>, and <b>death if untreated</b>."</p> <p>"<b>COMORBIDITY_INFO</b>": "Common complications include <b>neurological damage</b>, <b>liver dysfunction</b>, and <b>growth retardation</b>. Underlying causes are typically <b>genetic mutations affecting enzymes</b> in the urea cycle. Pathophysiological mechanisms involve the accumulation of ammonia and other toxic metabolites. Monitoring priorities should include <b>regular ammonia level checks</b>, <b>neurological assessments</b>, and <b>liver function tests</b> to prevent acute metabolic crises."</p>

Figure 4: The description of code 270.6 generated by GPT-4o.

### 3.3. Directed Bipartite Graph Encoder

In this module, we introduce the Directed Bipartite Graph Encoder for enhancing the representations of rare codes by aggregating latent comorbidity information from their co-occurring common counterparts.

#### 3.3.1. Graph Construction

As Figure 2 illustrates, the original code co-occurrence relationships are straightforward: two codes are connected if they co-occur within a document. We calculate a conditional probability metric between rare and common codes:

$$P(l_{c_j}|l_{r_i}) = \frac{N_{l_{r_i} \cap l_{c_j}}}{N_{l_{r_i}}} \quad (3)$$

Here,  $N_{l_{r_i} \cap l_{c_j}}$  represents the number of times rare code  $l_{r_i}$  and common code  $l_{c_j}$  co-occur, and  $N_{l_{r_i}}$  is the total occurrences of  $l_{r_i}$  in the training dataset. The conditional probability matrix is denoted as  $\mathbf{P} \in [0, 1]^{N_r \times N_c}$ , where  $N_r$  is the total number of rare codes and  $N_c$  is the total number of common codes.

The Directed Bipartite Graph is defined as  $\mathcal{G} = (\mathcal{V}, \mathcal{E})$ , where  $\mathcal{V} = \mathcal{V}_c \cup \mathcal{V}_r$  represents the set of ICD codes, and  $\mathcal{V}_c \cap \mathcal{V}_r = \emptyset$ . Here,  $\mathcal{V}_c = \{l_{c_j} : j \in \{1, 2, \dots, N_c\}\}$  denotes the set of common codes, with  $N_c$  being their total number, and  $\mathcal{V}_r = \{l_{r_i} : i \in \{1, 2, \dots, N_r\}\}$  denotes the set of rare code, with  $N_r$  being their total number. The edge set  $\mathcal{E}$  consists of directed edges from common codes to rare codes, facilitating information transmission.

### 3.3.2. Co-occurrence Encoding with Probability-based Bias

To effectively model the co-occurrence relationships between ICD codes, we introduce a novel “Co-occurrence Encoding.” This item is a domain-specific adaptation of the “Spatial Encoding” component in the graph Transformer model Graphormer [16].

While Transformer layers for sequential data explicitly model positional dependencies, often through methods like relative positional encoding [19, 20], graphs lack an inherent sequential arrangement. To address this, Graphormer incorporates a learnable “Spatial Encoding” bias within its attention module, indexed by the shortest path distance (SPD) between nodes. In the medical domain, however, the statistical co-occurrence of codes, which often reflects underlying comorbidity among diseases, serves as a powerful signal [6]. Consequently, our proposed bias is indexed not by distance, but by the conditional probability between code pairs. This allows our model to acquire a more fine-grained, representation-level understanding of co-occurrence relationships among codes.

The implementation of Co-occurrence Encoding involves discretizing continuous probability values into a fixed number of bins. The procedure for generating the bin index  $\varphi(l_{r_i}, l_{c_j})$  for any code pair is based on quantile binning (detailed in Algorithm 1).

The probability-based bias  $c_{\varphi(l_{r_i}, l_{c_j})}$  is a learnable scalar indexed directly by  $\varphi(l_{r_i}, l_{c_j})$ . This bias is then incorporated into the attention calculation for the  $k$ -th head ( $k \in 1, \dots, K$ , where  $K$  is the number of heads) between a rare  $l_{r_i}$  code and a common code  $l_{c_j}$  as follows:

$$A_{l_{r_i} l_{c_j}}^k = \text{SoftMax}_{l_{c_j} \in \mathcal{V}_c} \left( \frac{(V_{l_{r_i}} W_R^k)(V_{l_{c_j}} W_C^k)'}{\sqrt{d_k}} + c_{\varphi(l_{r_i}, l_{c_j})}^k + m_{l_{r_i}, l_{c_j}} \right) \quad (4)$$

Here,  $W_R$  and  $W_C$  are the projection matrices for the query and key of the  $k$ -th attention head, respectively, and  $d_k$  is the dimension of the query and key for the  $k$ -th head ( $d_k = d/K$ ). The probability-based bias for the  $k$ -th head is denoted as  $c_{\varphi(l_{r_i}, l_{c_j})}^k$ . The term  $m_{l_{r_i}, l_{c_j}}$  serves as a binary mask to control co-occurrence. Specifically, it is set to  $-\infty$  if codes  $l_{r_i}$  and  $l_{c_j}$  do not co-occur, effectively preventing attention between them. Conversely, it is set to 0 if they do co-occur, allowing common codes to transmit information to their co-occurring rare codes.

The output of the multi-head attention mechanism for the rare code  $l_{r_i}$  is then the concatenation of the outputs from all heads, followed by a linear

---

**Algorithm 1:** Binning for Probability-based Bias

---

**Input** : Conditional Probability Matrix  $\mathbf{P} \in \mathbb{R}^{N_r \times N_c}$ ; Bin number  $B$ .

**Output** : Bin indices  $\varphi(l_{r_i}, l_{c_j}) \in \{0, 1, \dots, B\}, i \in \{1, \dots, N_r\}, j \in \{1, \dots, N_c\}$

**Step 1: Quantile Binning with Zero Handling begin**

1. **Flatten matrix:**  $\mathbf{P}_{flat} \leftarrow \mathbf{P}.flatten()$
2. **Separate zeros:**  $\mathbf{P}_{nonzero} \leftarrow \mathbf{P}_{flat}[\mathbf{P}_{flat} \neq 0]$
3. **Compute quantiles: begin**
  - quantiles  $\leftarrow [0.0, 0.1, \dots, 1.0]$
  - bins  $\leftarrow \text{np.quantile}(\mathbf{P}_{nonzero}, \text{quantiles})$
4. **Merge boundaries:** bins  $\leftarrow \text{np.concatenate}([0.0], \text{bins})$

**Step 2: Index Assignment begin**

- for  $i \leftarrow 1$  to  $N_r$  do
  - for  $j \leftarrow 1$  to  $N_c$  do
    - if  $\mathbf{P}(i, j) = 1$  then
      - $\varphi(l_{r_i}, l_{c_j}) \leftarrow B$
    - else
      - $\varphi(l_{r_i}, l_{c_j}) \leftarrow \text{torch.bucketize}(\mathbf{P}(i, j), \text{bins}, \text{right}=\text{True}) - 1$

**return**  $\varphi$

---

transformation:

$$Att_{l_{r_i}} = W_{att} \cdot \text{Concat}(head_1, head_2, \dots, head_H) \quad (5)$$

where  $head_h = \sum_j A_{l_{r_i} l_{c_j}}^h V_{l_{c_j}} W_V^h$ ,  $W_V$  is the projection matrix for  $l_{c_j}$ , and  $W_{att}$  is the linear layer that combines the outputs of all heads. The resulting rare code attention features,  $Att_{l_{r_i}}$ , along with common code features,  $V_{l_{c_j}}$ , are then processed through a Dropout Layer, Normalization, Residual Connection, and MLP layers to generate the final graph encoder output,  $V^G = \{V_i^G\}$ , where  $i \in \{1, 2, \dots, N\}$  and  $N$  is the total number of codes. This feed-forward layer performs local refinement on all codes, which enhances the discriminative power of the output features and improves classification recognition capability.

### 3.4. Co-occurrence-Infused Multi-Label Attention

The multi-label attention mechanism is a prevalent technique in text classification and has been adapted by researchers for various task designs. Notable examples include ‘‘Hierarchy-Aware Multi-Label Attention’’ [21] and

“Multi-synonyms Attention” [7, 9], which in turn draw inspiration from the multi-head attention mechanism of the Transformer architecture [22]. To integrate the chunked document representation  $H = \{H^u\}$  with the comorbidity information infused code features  $V^G = \{V_i^G\}$  from the graph encoder, we implement a multi-label attention mechanism to extract text features specific to each code. While our implementation utilizes multi-head attention, for clarity of presentation, the following equations illustrate the computation for a single head. First, let the document chunk representation  $H^u \in \mathbb{R}^{T \times d}$  be a sequence of token representations  $H^u = \{h_1^u, h_2^u, \dots, h_T^u\}$ , where  $h_t^u \in \mathbb{R}^d$  is the representation for the  $t$ -th token. The code features  $V_i^G$  are then used to query this token sequence as follows:

$$\alpha_u^i = \text{SoftMax}_{t \in 1, \dots, T} ((W_Q V_i^G) \cdot \text{Tanh}(W_K h_t^u)^T) \quad (6)$$

Here,  $W_Q$  and  $W_K$  are projection matrices, and  $\alpha_u^i \in \mathbb{R}^T$  quantifies the attention of code  $l_i$  across the tokens of the  $u$ -th document chunk  $X_u$ . We leverage this attention distribution as weights to compute a code-specific representation for the current chunk.

$$R_u^i = \sum_{t=1}^T \alpha_{u,t}^i H_t^u \quad (7)$$

For classification of the document  $H$ , we employ a biaffine transformation with the derived chunk-level representation  $R_u^i$ :

$$\hat{y}_i = \sigma(\text{MaxPool}_u(R_u^i W V_i^G)). \quad (8)$$

In this equation, the  $\text{MaxPool}_u$  operation aggregates representations across all  $U$  chunks into a unified document-level score.  $\sigma$  is the sigmoid activation, providing the probability  $\hat{y}_i$  for code  $l_i$ .

### 3.5. Binary Cross-Entropy Loss Function

For model training, we employed the widely-used Binary Cross-Entropy (BCE) loss. This loss function is averaged over all samples within a batch. For a single document, the BCE loss is defined as:

$$\mathcal{L}_{BCE} = -\frac{1}{N} \sum_{i=1}^N [y_i \log(\hat{y}_i) + (1 - y_i) \log(1 - \hat{y}_i)] \quad (9)$$

Where  $N$  is the total number of codes.

## 4. Experiments

### 4.1. Dataset

Our experiments are conducted on the full versions of three benchmark datasets: MIMIC-III-ICD-9, MIMIC-IV-ICD-9, and MIMIC-IV-ICD-10. These datasets are derived from the MIMIC-III [23] and MIMIC-IV [24] clinical databases, which we accessed via PhysioNet<sup>5</sup> after completing the required ethical training program. We adopt the widely-used data splits and processing procedures in [25] for MIMIC-III, and [2] for the two MIMIC-IV datasets (see Table 1, 2, and 3 for statistics), ensuring a comprehensive evaluation on the complete, long-tail label space.

Table 1: Statistics of the MIMIC-III-ICD-9 dataset.

Statistics	MIMIC-III-ICD-9			
	All	Train	Dev	Test
Number of Documents.	52,726	47,723	1,631	3,372
Average Number of Tokens per Document.	2,768	2,707	3,338	3,360
Average Number of Codes per Document.	15.9	15.7	17.4	18.0
Total Number of Codes.	8,921	8,685	3,009	4,075

Table 2: Statistics of the MIMIC-IV-ICD-9 dataset.

Statistics	MIMIC-IV-ICD-9			
	All	Train	Dev	Test
Number of Documents.	209,352	188,533	7,110	13,709
Average Number of Tokens per Document.	1,693	1,693	1,708	1,695
Average Number of Codes per Document.	13.3	13.3	13.5	13.3
Total Number of Codes.	11,331	11,145	5,115	6,264

Table 3: Statistics of the MIMIC-IV-ICD-10 dataset.

Statistics	MIMIC-IV-ICD-10			
	All	Train	Dev	Test
Number of Documents.	122,309	110,441	4,017	7,851
Average Number of Tokens per Document.	1,956	1,958	1,968	1,931
Average Number of Codes per Document.	16.1	16.1	16.2	15.8
Total Number of Codes.	26,096	25,230	6,738	9,159

<sup>5</sup><https://physionet.org/>

We categorize codes as “rare” based on their frequency in the training data. The frequency threshold is set to  $<10$  for MIMIC-III-ICD-9 and MIMIC-IV-ICD-10, and  $<100$  for MIMIC-IV-ICD-9. This definition places a significant portion of codes (approx. 70%) into the rare category (see Figure 5). The segmentation strategy follows studies in other domains that focus on the long-tail label space [26, 27, 28, 29].

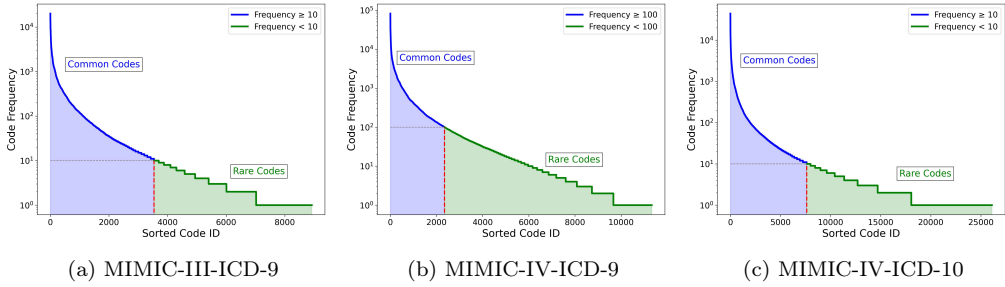


Figure 5: The power-law label distribution of three benchmark datasets. We sort the label IDs in descending order with reference to the number of related documents.

#### 4.2. Baselines and Evaluation Metrics

We compare our model with existing outstanding methods. Following are the baselines:

CAML: It aggregates information across the document through a convolutional neural network and an attention module [25].

LAAT: It handles both the various lengths and the interdependence of the ICD code related text fragments [30].

JointLAAT: It minimizes the joint losses of both parent and child codes from code ontology to address long-tail distribution [30].

MSMN: It proposes a multiple synonyms matching network to leverage synonyms for better code representation learning [7].

PLM-ICD: It develops a framework for automatic ICD coding with pre-trained language models [31].

CoRelation: It employs a dependent learning paradigm that considers the context of clinical notes in modeling all possible code relations [4].

MSAM: It employs a selection algorithm to choose a more distinct subset of synonyms for each code [9].

Following these studies, we evaluate our model ProBias using a comprehensive set of metrics: Macro/Micro AUC, Macro/Micro F1, and Precision@8.

We place special emphasis on Macro F1, as it averages per-class scores, making it a crucial indicator of a model’s performance on rare classes within the long-tail distribution.

#### *4.3. Implementation Details*

We conducted all experiments on a single NVIDIA H100 GPU with 80GB of memory. Our model’s training hyper-parameters remained consistent across all three datasets.

For input processing, we set the maximum input length to 6122 tokens, dividing them into 512-token chunks with an overlapping window of 255. The GatorTron’s hidden size was 1,024. The attention mechanism within the graph utilized a hidden size of 512 and 4 heads. The feed-forward layer included a dropout rate of 0.1, and the linear layer in it also had a hidden size of 512. To enhance computational efficiency and reduce GPU memory consumption, we trained our model using BFloat16 precision. We optimized our model with AdamW, employing a starting learning rate of  $2e-5$  and a linear decay schedule. To prevent overfitting, early stopping was applied based on the Macro F1 score on the validation set. Our model was trained for 15 epochs with a batch size of 1 and 16 gradient accumulation steps.

#### *4.4. Main Results*

As demonstrated in Table 4, 5, and 6, our model, ProBias, achieves new state-of-the-art (SOTA) results across all three benchmark datasets. On MIMIC-III-ICD-9, ProBias substantially outperforms other methods, boosting the Macro F1 score from 11.4 to 14.2 (a 2.8-point improvement). This superiority continues on the more recent MIMIC-IV datasets. Specifically, on MIMIC-IV-ICD-9, ProBias improves the SOTA Macro F1 score from 15.9 to 18.6, and on MIMIC-IV-ICD-10, it lifts the Macro F1 from 6.3 to 7.7.

The substantial improvements in Macro F1 across all datasets are particularly noteworthy. This metric is crucial for evaluating performance on long-tail distributions, as it is highly sensitive to a model’s effectiveness on rare classes, thus validating our model’s superior ability to handle the long-tail challenge. Concurrently, strong results in both Micro F1 and Precision@8 confirm the model’s high overall accuracy and its capacity to rank the most relevant labels effectively.

Table 4: Performance comparison with baseline models on MIMIC-III-ICD-9 dataset. Our ProBias results represent the average of five runs with different random seeds. Baseline results are taken from their original publications, with the exception of MSAM, which we reproduced using the public code. The best results are highlighted in **Bold**.

Method	AUC		F1		Pre
	Macro	Micro	Macro	Micro	P@8
CAML [25]	89.5	98.6	8.8	53.9	70.9
LAAT [30]	91.9	98.8	9.9	57.5	73.8
JointLAAT [30]	92.1	98.8	10.7	57.5	73.5
MSMN [7]	95.0	<b>99.2</b>	10.3	58.4	75.2
PLM-ICD [31]	92.6	98.9	10.4	59.8	<b>77.1</b>
CoRalation [4]	95.2	<b>99.2</b>	10.2	59.1	76.2
MSAM [9]	94.6	99.1	11.4	59.2	75.9
ProBias (ours)	<b>95.3</b>	<b>99.2</b>	<b>14.2</b>	<b>60.8</b>	77.0

Table 5: Performance comparison with baseline models on MIMIC-IV-ICD-9 dataset. Our ProBias results represent the average of five runs with different random seeds. Baseline results are from Luo et al. [4], with the exception of MSAM, which we reproduced using the public code. The best results are highlighted in **Bold**.

Method	AUC		F1		Pre
	Macro	Micro	Macro	Micro	P@8
CAML [25]	93.5	99.3	11.1	57.3	64.9
LAAT [30]	95.2	99.5	13.1	60.3	67.5
JointLAAT [30]	95.6	99.5	14.2	60.4	67.5
MSMN [7]	96.8	<b>99.6</b>	13.9	61.2	68.9
PLM-ICD [31]	96.6	99.5	14.4	62.5	70.3
CoRalation [4]	96.8	99.5	15.0	62.4	70.1
MSAM [9]	<b>97.5</b>	<b>99.6</b>	15.9	<b>63.2</b>	<b>71.0</b>
ProBias (ours)	<b>97.5</b>	<b>99.6</b>	<b>18.6</b>	<b>63.2</b>	70.5

#### 4.5. Analysis of Key Hyperparameters

We conducted experiments on the MIMIC-III-ICD-9 dataset to determine the optimal settings for key hyperparameters, specifically the number of bins for our Co-occurrence Encoding and the number of layers in the Directed Bipartite Graph Encoder.

As shown in Table 7, we evaluated bin numbers of 5, 10, and 15. A setting of 10 was chosen as it achieved the best Macro F1 score (14.2), providing an optimal balance between information granularity and model generalization. For the number of graph layers (see Table 8), we ultimately selected a single-layer architecture. While a 2-layer model yielded a marginally higher Macro F1 score (14.4 vs. 14.2), the single-layer configuration is significantly more efficient in terms of computational resources, a crucial consideration for



Table 6: Performance comparison with baseline models on MIMIC-IV-ICD-10 dataset. Our ProBias results represent the average of five runs with different random seeds. Baseline results are from Luo et al. [4], with the exception of MSAM, which we reproduced using the public code. The best results are highlighted in **Bold**.

Method	AUC		F1		Pre
	Macro	Micro	Macro	Micro	P@8
CAML [25]	89.9	98.8	4.1	52.7	64.4
LAAT [30]	93.0	99.1	4.5	55.4	67.0
JointLAAT [30]	93.6	99.3	5.7	55.9	66.9
MSMN [7]	97.1	99.6	5.4	55.9	67.7
PLM-ICD [31]	91.9	99.0	4.9	57.0	69.5
CoRation [4]	97.2	99.6	6.3	57.8	70.0
MSAM [9]	<b>97.7</b>	<b>99.7</b>	6.3	58.5	<b>70.4</b>
ProBias (ours)	97.3	99.6	<b>7.7</b>	<b>58.7</b>	70.0

scalability to larger datasets (e.g., MIMIC-IV-ICD-10). Given the consistency of the three datasets in terms of domain and features, we adopted the same hyperparameter settings across them.

Table 7: Performance comparison of different bin number in Co-occurrence Encoding (5, 10 and 15) on MIMIC-III-ICD-9 dataset. The best results are highlighted in **Bold**.

Models	AUC		F1		Pre		
	Macro	Micro	Macro	Micro	P@5	P@8	P@15
ProBias ( $b_5$ )	<b>95.6</b>	<b>99.3</b>	13.7	60.5	83.5	76.6	61.9
ProBias ( $b_{10}$ )	95.3	99.2	<b>14.2</b>	<b>60.8</b>	<b>84.0</b>	<b>77.0</b>	<b>62.0</b>
ProBias ( $b_{15}$ )	95.3	99.2	13.8	60.3	83.4	76.6	61.6

Table 8: Performance comparison of different layer number in Directed Bipartite Graph Encoder (1, 2 and 3) on MIMIC-III-ICD-9 dataset. The best results are highlighted in **Bold**.

Models	AUC		F1		Pre		
	Macro	Micro	Macro	Micro	P@5	P@8	P@15
ProBias ( $l_1$ )	95.3	99.2	14.2	<b>60.8</b>	<b>84.0</b>	<b>77.0</b>	<b>62.0</b>
ProBias ( $l_2$ )	95.3	99.2	<b>14.4</b>	60.5	83.4	76.7	61.8
ProBias ( $l_3$ )	<b>95.5</b>	<b>99.3</b>	14.3	60.6	83.6	76.7	61.9

#### 4.6. Ablation Study

The model’s design is validated through a series of ablations (see Table 9): ProBias(MI) serves as the baseline, using a simple adjacency graph with Mutual Information flow between all co-occurring codes. ProBias(DI) refines

this by introducing **D**irectional **I**nformation flow from common to co-occurring rare codes. ProBias(CE) implements our core contribution by upgrading this directional information flow to the fine-grained **C**o-occurrence **E**ncoding with probability-based bias. Finally, ProBias(CE+des), the full model, where “des” denotes descriptions generated by LLM substituting code names as graph input, achieves the best results.

Table 9: Performance comparison of different ablation versions. The best results are highlighted in **Bold**.

Models	AUC		F1		Pre		
	Macro	Micro	Macro	Micro	P@5	P@8	P@15
ProBias (MI)	95.5	99.2	11.8	60.0	83.2	76.1	61.4
ProBias (DI)	95.6	<b>99.3</b>	12.4	60.4	84.0	76.9	61.7
ProBias (CE)	<b>95.7</b>	<b>99.3</b>	13.3	60.7	<b>84.3</b>	<b>77.2</b>	<b>62.0</b>
ProBias (CE+des)	95.3	99.2	<b>14.2</b>	<b>60.8</b>	84.0	77.0	<b>62.0</b>

The base version, ProBias(MI), already provides a strong performance foundation, attributable to the entire well-designed pipeline. Building on this, the incremental improvements from ProBias(MI) to ProBias(DI), ProBias(CE), and finally to ProBias(CE+des), validate the importance of each subsequent component: our Directed Bipartite Graph structure, the fine-grained Co-occurrence Encoding, and the external knowledge from the large language model.

## 5. Conclusion and Future Work

In this paper, we introduce ProBias, a Directed Bipartite Graph Encoder that addresses the long-tail problem in ICD coding by injecting a probability-based bias derived from co-occurrence statistics into the attention module to enrich rare code representations. To ensure high-quality input for the graph encoder, we utilize a large language model to generate comprehensive code descriptions. Experiments on three benchmark datasets demonstrate ProBias achieves state-of-the-art performance.

With regard to future work, while our core Co-occurrence Encoding component relies on discretizing continuous probability values through binning, we could explore a learnable mapping function that operates directly on these continuous values. For instance, a small multi-layer perceptron (MLP) could be used to transform probability values into a bias term, which will enable more precise capture of the subtle variations in comorbidity strength.

Besides, although LLM-generated code descriptions have enhanced long-tail performance, a promising direction is to integrate a gating mechanism to dynamically fuse these LLM-derived descriptions with original code names or ontological concepts (e.g., from UMLS). This approach would combine the descriptive richness of LLMs with the precision of formalized data, thereby further boosting the performance of this component.

### **Acknowledgment**

This work is supported by National Natural Science Foundation of China (No.72371241), the MOE Project of Key Research Institute of Humanities and Social Sciences (22JJD910001), and the Big Data and Responsible Artificial Intelligence for National Governance, Renmin University of China.

## References

- [1] L. S. Larkey, W. B. Croft, Combining classifiers in text categorization, in: Proceedings of the 19th annual international ACM SIGIR conference on Research and development in information retrieval, 1996, pp. 289–297.
- [2] T.-T. Nguyen, V. Schlegel, A. Kashyap, S. Winkler, S.-S. Huang, J.-J. Liu, C.-J. Lin, Mimic-iv-icd: A new benchmark for extreme multilabel classification, arXiv preprint arXiv:2304.13998 (2023).
- [3] P. Cao, Y. Chen, K. Liu, J. Zhao, S. Liu, W. Chong, Hypercore: Hyperbolic and co-graph representation for automatic icd coding, in: Proceedings of the 58th Annual Meeting of the Association for Computational Linguistics, 2020, pp. 3105–3114.
- [4] J. Luo, X. Wang, J. Wang, A. Chang, Y. Wang, F. Ma, Corelation: Boosting automatic icd coding through contextualized code relation learning, in: Proceedings of the 2024 Joint International Conference on Computational Linguistics, Language Resources and Evaluation (LREC-COLING 2024), 2024, pp. 3997–4007.
- [5] X. Wang, R. Mercer, F. Rudzicz, Multi-stage retrieve and re-rank model for automatic medical coding recommendation, in: Proceedings of the 2024 Conference of the North American Chapter of the Association for Computational Linguistics: Human Language Technologies (Volume 1: Long Papers), 2024, pp. 4881–4891.
- [6] J. M. Valderas, B. Starfield, B. Sibbald, C. Salisbury, M. Roland, Defining comorbidity: Implications for understanding health and health services, *The Annals of Family Medicine* 7 (2009) 357–363.
- [7] Z. Yuan, C. Tan, S. Huang, Code synonyms do matter: Multiple synonyms matching network for automatic icd coding, in: Proceedings of the 60th Annual Meeting of the Association for Computational Linguistics (Volume 2: Short Papers), 2022, pp. 808–814.
- [8] Z. Yang, S. Wang, B. P. S. Rawat, A. Mitra, H. Yu, Knowledge injected prompt based fine-tuning for multi-label few-shot icd coding, in: Proceedings of the conference on empirical methods in natural language processing. Conference on empirical methods in natural language processing, volume 2022, NIH Public Access, 2022, p. 1767.

- [9] G. Gomes, I. Coutinho, B. Martins, Accurate and well-calibrated icd code assignment through attention over diverse label embeddings, in: Proceedings of the 18th Conference of the European Chapter of the Association for Computational Linguistics (Volume 1: Long Papers), 2024, pp. 2302–2315.
- [10] Z. Yang, S. Kwon, Z. Yao, H. Yu, Multi-label few-shot icd coding as autoregressive generation with prompt, in: Proceedings of the AAAI Conference on Artificial Intelligence, volume 37, 2023, pp. 5366–5374.
- [11] T.-T. Nguyen, V. Schlegel, A. R. Kashyap, S. Winkler, A two-stage decoder for efficient icd coding, in: Findings of the Association for Computational Linguistics: ACL 2023, 2023, pp. 4658–4665.
- [12] T. N. Kipf, M. Welling, Semi-supervised classification with graph convolutional networks, in: International Conference on Learning Representations, 2017.
- [13] A. Rios, R. Kavuluru, Few-shot and zero-shot multi-label learning for structured label spaces, in: Proceedings of the conference on empirical methods in natural language processing. Conference on empirical methods in natural language processing, volume 2018, 2018, p. 3132.
- [14] X. Xie, Y. Xiong, P. S. Yu, Y. Zhu, Ehr coding with multi-scale feature attention and structured knowledge graph propagation, in: Proceedings of the 28th ACM international conference on information and knowledge management, 2019, pp. 649–658.
- [15] V. P. Dwivedi, X. Bresson, A generalization of transformer networks to graphs, arXiv preprint arXiv:2012.09699 (2020).
- [16] C. Ying, T. Cai, S. Luo, S. Zheng, G. Ke, D. He, Y. Shen, T.-Y. Liu, Do transformers really perform badly for graph representation?, Advances in neural information processing systems 34 (2021) 28877–28888.
- [17] X. Yang, A. Chen, N. PourNejatian, H. C. Shin, K. E. Smith, C. Parisien, C. Compas, C. Martin, M. G. Flores, Y. Zhang, et al., Gatortron: A large clinical language model to unlock patient information from unstructured electronic health records, arXiv preprint arXiv:2203.03540 (2022).

- [18] N. F. Liu, K. Lin, J. Hewitt, A. Paranjape, M. Bevilacqua, F. Petroni, P. Liang, Lost in the middle: How language models use long contexts, *Transactions of the Association for Computational Linguistics* 12 (2024) 157–173.
- [19] P. Shaw, J. Uszkoreit, A. Vaswani, Self-attention with relative position representations, in: *Proceedings of the 2018 Conference of the North American Chapter of the Association for Computational Linguistics: Human Language Technologies, Volume 2 (Short Papers)*, 2018, pp. 464–468.
- [20] C. Raffel, N. Shazeer, A. Roberts, K. Lee, S. Narang, M. Matena, Y. Zhou, W. Li, P. J. Liu, Exploring the limits of transfer learning with a unified text-to-text transformer, *Journal of machine learning research* 21 (2020) 1–67.
- [21] J. Zhou, C. Ma, D. Long, G. Xu, N. Ding, H. Zhang, P. Xie, G. Liu, Hierarchy-aware global model for hierarchical text classification, in: *Proceedings of the 58th annual meeting of the association for computational linguistics*, 2020, pp. 1106–1117.
- [22] A. Vaswani, N. Shazeer, N. Parmar, J. Uszkoreit, L. Jones, A. N. Gomez, L. Kaiser, I. Polosukhin, Attention is all you need, in: *Proc. of the 31st Int. Conference on Neural Information Processing Systems*, 2017, pp. 6000–6010.
- [23] A. Johnson, T. Pollard, R. Mark, MIMIC-III Clinical Database (version 1.4), <https://doi.org/10.13026/C2XW26>, 2016. Accessed: 2024-08-28.
- [24] A. Johnson, T. Pollard, S. Horng, L. A. Celi, R. Mark, MIMIC-IV-Note: Deidentified free-text clinical notes (version 2.2), <https://doi.org/10.13026/1n74-ne17>, 2023. Accessed: 2024-08-28.
- [25] J. Mullenbach, S. Wiegrefe, J. Duke, J. Sun, J. Eisenstein, Explainable prediction of medical codes from clinical text, in: *Proceedings of the 2018 Conference of the North American Chapter of the Association for Computational Linguistics: Human Language Technologies, Volume 1 (Long Papers)*, 2018, pp. 1101–1111.
- [26] Y.-X. Wang, D. Ramanan, M. Hebert, Learning to model the tail, *Advances in neural information processing systems* 30 (2017).

- [27] Z. Liu, Z. Miao, X. Zhan, J. Wang, B. Gong, S. X. Yu, Large-scale long-tailed recognition in an open world, in: Proceedings of the IEEE/CVF conference on computer vision and pattern recognition, 2019, pp. 2537–2546.
- [28] L. Xiao, X. Zhang, L. Jing, C. Huang, M. Song, Does head label help for long-tailed multi-label text classification, in: Proceedings of the AAAI conference on artificial intelligence, volume 35, 2021, pp. 14103–14111.
- [29] H. Wang, C. Peng, H. Dong, L. Feng, W. Liu, T. Hu, K. Chen, G. Chen, On the value of head labels in multi-label text classification, ACM Transactions on Knowledge Discovery from Data 18 (2024) 1–21.
- [30] T. Vu, D. Q. Nguyen, A. Nguyen, A label attention model for icd coding from clinical text, in: Proceedings of the Twenty-Ninth International Conference on International Joint Conferences on Artificial Intelligence, 2021, pp. 3335–3341.
- [31] C.-W. Huang, S.-C. Tsai, Y.-N. Chen, Plm-icd: Automatic icd coding with pretrained language models, in: Proceedings of the 4th Clinical Natural Language Processing Workshop, 2022, pp. 10–20.